THE 4TH INTERNATIONAL CONFERENCE ON ALUMINUM ALLOYS

TENSILE FRACTURE OF A 2090 EXTRUSION

William D. Pollock and Stephen J. Hales
Analytical Services and Materials, Inc., 107 Research Drive,
Hampton, VA 23666, USA.

Abstract

The structure-property-processing relationship of a 2090 near-net-shape extrusion in the T86 temper has been evaluated. The study revealed that both the microstructure and the tensile behavior are strongly dependent on the local extrusion aspect ratio. Regions of low extrusion aspect ratio within the cross-section comprised a fibrous microstructure and exhibited the highest yield strength. Regions of high extrusion aspect ratio exhibited a pancake-shaped grain morphology and tensile behavior comparable to 2090 sheet. Fractographic analyses suggested that macroscopic fracture mode was closely related to local grain morphology. Microscopically, the fracture characteristics were consistent with inter-(sub)granular failure. The influence of microstructure on tensile properties and fracture behavior as a function of location and orientation were addressed.

Introduction

Aluminum lithium (Al-Li) alloys offer a high strength, low density alternative to 2219, the alloy used in the fabrication of the Space Shuttle External Tank [1]. The potential exists to reduce the high manufacturing costs associated with the current integrally machined, T-stiffened design by using near-net-shape forming techniques [2]. Production-scale billets of alloy 2090 were extruded into integrally stiffened tubes which were then cut along the length and roll-flattened. The final product comprised L-stiffened panels 0.825m wide and 3.0m long with a skin thickness of 4.5mm and stiffeners 116mm apart. The individual stiffeners were 33mm high, 21mm wide and 5.6mm thick. The material evaluated in this study had the composition Al -2.7Cu -2.1Li -0.12Zr -0.09Fe -0.05Si -0.03Ti (wt.%) and was in a T86 temper (6% stretched + peak aged) condition [3]. The objective was to correlate microstructure with tensile behavior as a function of location and orientation in the extruded cross-section.

The microstructure and tensile properties of near-net-shape extrusions are dependent on both forming conditions and component geometry [4-8]. The key parameters are the extrusion ratio ($Area_{Billet}$: $Area_{Extrusion}$), and the extrusion aspect ratio (Width : Thickness, W/T), which will vary with cross-section. The overall extrusion ratio for the cross-section was $\approx$ 9:1, which is lower than that typically employed ($\geq$ 20:1) for Al-Li alloys [3]. It has been demonstrated that

increasing the extrusion ratio promotes recrystallization and less anisotropic tensile behavior in 8090 extrusions [5]. The extrusion aspect ratio varied from W/T $\approx$ 4 in the stiffeners to W/T $\approx$ 30 in the skin. Fibrous (cigar-shaped) and pancake-shaped grain structures are common in regions of low and high W/T forming, respectively [6]. The trend in tensile behavior is toward a decrease in yield strength and more isotropic properties with increasing W/T [7]. In Al-Li extruded product, variations in grain structure tend to contribute less to property anisotropy than changes in texture [8].

Experimental Procedures

The nomenclature adopted to indicate the locations in the cross-section which were characterized is outlined in Figure 1(a). Longitudinal (L) specimens were tested at each position (skin, base, web and cap), long transverse (LT) specimens in the base and skin, and 45° specimens in the skin. Tensile testing conformed with ASTM B 557M specifications, using standard, sub-sized coupons [9]. Elongation-to-failure was measured over a 25mm gauge length using extensometers and the plastic strain was calculated by subtracting the elastic strain from the total strain.

Optical metallography was performed to study the grain structure as a function of location and orientation in the extruded cross-section. Metallographic samples were anodized using Barker's reagent and imaged under cross-polarized light. Fractographic samples were examined visually to assess macroscopic fracture mode. Scanning electron microscopy was employed to evaluate the microscopic failure mechanisms. Metallographic sections perpendicular to fracture surfaces were also examined to correlate macroscopic with microscopic features.

Results and Discussion

Microstructure

The microstructural characteristics of the 2090 near-net-shape extrusion were similar to those of other Al-Li products extruded with a low extrusion ratio [4,5]. The unrecrystallized microstructure was highly elongated parallel to the extrusion axis and contained a subgrain structure with a more equiaxed morphology than the grains [7]. The aspect ratio of the unrecrystallized grains in the plane perpendicular to the extrusion axis reflected the local changes in extrusion aspect ratio, W/T. The variations in grain structure with location in the cross-section are summarized schematically in Figure 1(a). The grain morphology was fibrous in the cap and exhibited features characteristic of an axisymmetric extrusion (W/T $\approx$ 1) [6,7]. In contrast, the pancake-shaped grain morphology in the skin, with W/T » 1, was similar to the microstructure of unrecrystallized 2090 sheet [8,10].

The microstructures present in the cap and the bulk of the skin were relatively homogeneous through the cross-section. The web and base regions exhibited distinctly heterogeneous microstructures, which comprised a combination of grain structures. The microstructural characteristics of the web and base are illustrated in Figures 1(b)-1(e). The web contained areas of pancake-shaped grains with distinctly different alignments in the plane perpendicular to the extrusion axis. Adjacent to both surfaces of the web, the grains were inclined towards the center, as illustrated in Figure 1(b). An area of pancake-shaped grains aligned perpendicular to the skin separated these regions, as shown in Figure 1(c). This region was offset from the

centerline of the web on the cap side of the stiffener. Comparing Figures 1(b) with 1(c) reveals that the grains in the middle possessed a lower aspect ratio than the inclined grains at the surfaces.

The base exhibited a microstructure which contained an arrangement of grain structures with different morphologies and varying alignment. Adjacent to the surface opposite the stiffener (below area "e" in Figure 1(a)), the grains were pancake-shaped with similar aspect ratio and alignment to that in the skin. At the intersection of the stiffener with the skin, Figure 1(d), the pancake-shaped grains were aligned with the contour of each fillet. The aspect ratio of these grains tended to decrease with proximity to the center of the base region. At approximately the center, Figure 1(e), the microstructure consisted of a mixture of fibrous and pancake-shaped grains.

B. Tensile Behavior

Tensile properties as a function of location and orientation across the 2090 near-net-shape extrusion are presented in Figure 2. The highest strength was associated with L base and L cap where the properties appear to be related to the presence of the fibrous grain structure. The L skin and L web specimens exhibited lower strength and elongation to failure than L base and L cap. The similarity in properties of the skin and web resulted from the abundance of the pancake-shaped grain structure in both regions. As a function of orientation in the skin, LT skin was stronger and marginally more ductile than L skin, while 45°skin exhibited high elongation-to-failure, but low strength. The level of anisotropy observed was consistent with the domination of texture effects in unrecrystallized Al-Li wrought product [11,12]. The variation in tensile properties with orientation was comparable with the behavior documented for both 2090 sheet and 8090 extrusions [7,10].

In the base material, the arrangement of the different grain structures relative to the tensile axis may have contributed to the anisotropy in behavior. In L base specimens, the elongated microstructure was parallel to the tensile axis, with the fibrous and pancake-shaped grains arranged across the gage length. Deformation involved each of the microstructural components and the dominance of the fibrous grain structure, which exhibited high yield strength in L cap, was considered responsible for the high strength. In LT base specimens, the elongated microstructure was perpendicular to the tensile axis, with the fibrous and pancake-shaped grains arranged along the gage length. The strength of LT base was comparable to LT skin, which possessed the pancake-shaped grain morphology. This suggests that the pancake-shaped grains had a stronger influence on tensile behavior than the fibrous grains.

C. Fracture Behavior

(i) Macroscopic Features. The macroscopic fracture behavior was dependent on the local microstructural characteristics and varied across the extruded cross-section. During deformation of specimens in the L orientation, the long dimension of the highly elongated grains was parallel to the tensile axis. In L skin specimens, which consisted entirely of a pancake-shaped grain structure, a single slant fracture traversed the gage section. Failure of the L cap specimens comprised 'mixed mode' fracture, with small 'shear' lips to each side of the gage section. The whole microstructure at this location consisted of a fibrous grain morphology. In this context, the term 'mixed mode' infers failure along a plane perpendicular to loading by a mixture of flat and slant fracture.

In L base specimens, failure occurred by a combination of mixed mode and slant fracture, corresponding to the regions of fibrous and pancake-shaped grains, respectively. Mixed mode fracture of the fibrous grains constituted the center of the failure and multiple slant fracture surfaces tended to follow the various grain alignments in the underlying microstructure. Failure of the L web specimens, was by a mixture of mixed mode and slant fracture. The pancake-shaped grains with lower aspect ratio near the center exhibited mixed mode fracture, whereas the inclined grain structures adjacent to the web surface exhibited slant fracture.

The macroscopic fracture behavior also varied with orientation in the extrusion. In comparison to the single slant fracture of L skin, the fracture surfaces of LT skin and 45° skin specimens exhibited mixed mode fracture. LT skin failed in a similar manner to L cap with mixed mode fracture at the center and 'shear' lips toward the edges. In LT base specimens, failure occurred within the pancake-shaped grains adjacent to the fillets and did not traverse the fibrous microstructure at the center of the gauge length. The transition from mixed mode to slant fracture is shown in Figure 3 for LT base. The micrograph and accompanying schematic show that the macroscopic fracture characteristics can be correlated with microscopic features. The direction of crack propagation during slant fracture followed the local grain alignment around the fillet.

(ii) Microscopic Features. Microscopically, fracture of the tensile specimens tended to follow the local alignment of boundaries in the underlying grain structure. The correlation between microscopic fracture features and microstructure is illustrated for L cap and LT skin in Figures 4 and 5, respectively. A fracture surface typical of cap material with the tensile axis in the L orientation is shown in Figure 4(a). The surface was dominated by features which were equiaxed in the plane perpendicular to the extrusion axis. At this location and in this orientation, the tensile axis was parallel to the long dimension of the fibrous grain structure. As shown in Figure 4(b), the fracture features correlate well with the equiaxed morphology of the grains perpendicular to the extrusion axis.

A fracture surface typical of skin material with the tensile axis oriented in the LT direction is shown in Figure 5(a). The surface comprised relatively smooth features, highly elongated parallel to the extrusion axis (L). In LT skin specimens, the long dimension of the pancake-shaped grains was oriented perpendicular to the tensile direction. Figure 5(b) indicates that the shape of the fracture features was closely related to the elongated morphology of the underlying (sub)grain structure. The scale of the features observed on the fracture surfaces of both L cap and LT skin specimens suggested failure along both grain and subgrain boundaries [13-15].

Conclusions

1. As a function of position in the extruded cross-section, grain morphology and tensile properties were dependent on the local extrusion aspect ratio, W/T;
   (a) Low W/T (cap) resulted in a fibrous microstructure and strength similar to an axisymmetric extrusion.
   (b) High W/T (base) resulted in a pancake-shaped grain structure and tensile behavior comparable to 2090 sheet.

2. Arrangement of the different grain structures in the base influenced the tensile behavior;
   (a) With the microstructural components arranged parallel to the tensile axis (L base), properties were dominated by the fibrous grain structure.
   (b) With the microstructural components arranged perpendicular to the tensile axis (LT base), behavior was influenced by the pancake-shaped grains.

3. Macroscopic failure of the extruded material comprised mixed mode fracture. Microscopically, fracture of tensile specimens was influenced by local grain morphology. Independent of location and orientation, the fracture characteristics were consistent with inter-(sub)granular failure.

Acknowledgements

This research was conducted in the Materials Division at NASA Langley Research Center under contract NAS1-19708 with Mr. John A. Wagner as technical monitor.

References

1. T. Kaminski, et al.; *Aluminium-Lithium*, ed. M. Peters and P.-J. Winkler (Oberursel, Germany: Deutsche Gesellschaft fur Materialkunde e.V., 1992), 1311-16.
2. H. Kudo; J. Materials Processing Technology, 22 (1990), 307-42.
3. M.J. Birt, et al.; ***The Characterization of a 2090 Al-Cu-Li Alloy Near Net Shape Extrusion***, NASA Technical Memorandum, Langley Research Center, Hampton, VA (1994), in press.
4. M.J. Tan and T. Sheppard; ***4th International Aluminium Lithium Conference***, ed. G. Champier et al. (Les Ulis, France: Les Editions de Physique, 1987), 209-18.
5. N.C. Parson and T. Sheppard; *Aluminium-Lithium Alloys III*, ed. C. Baker et al. (London: The Institute of Metals, 1986), 222-32.
6. M.H. Skillingberg and R.F. Ashton; ***4th International Aluminium Lithium Conference***, ed. G. Champier et al. (Les Ulis, France: Les Editions de Physique, 1987), 179-86.
7. G. Tempus, W. Calles, and G. Scharf; J. Mater. Sci. Tech., 7 (1991), 937-45.
8. M.A. Reynolds and E. Creed; ***4th International Aluminium Lithium Conference***, ed. G. Champier et al. (Les Ulis, France: Les Editions de Physique, 1987), 195-207.
9. *Annual Book of ASTM Standards: Metals - Mechanical Testing*; Vol. 3.01 (Philadelphia, PA: ASTM, 1989), 64.
10. I.G. Palmer, et al.; *Aluminium-Lithium Alloys III*, ed. C. Baker et al. (London: The Institute of Metals, 1986), 565-75.
11. W.E. Quist and G.H. Narayanan; *Aluminum Alloys - Contemporary Research and Applications*, ed. A.K. Vasudevan and R.D. Doherty (San Diego: Academic Press, 1989), 219-54.
12. R.S. James; *Properties and Selection: Nonferrous Alloys and Pure Metals*, 10th Ed. Metals Handbook, Vol. 2 (Metals Park, OH: ASM International, 1990), 178-99.
13. D. Dew-Hughes, E. Creed, and W.S. Miller; J. Mater. Sci. Tech., 4 (1988), 106-12.
14. R.C. Dorwood; *Advances in Fracture Research*, ed. K. Salama et al. (New York: Pergamon Press, 1989), 2413-22.
15. E.J. Lavernia, T.S. Srivatsan and F.A. Mohamed; J. Mat. Sci., 25 (1990), 1137-58.

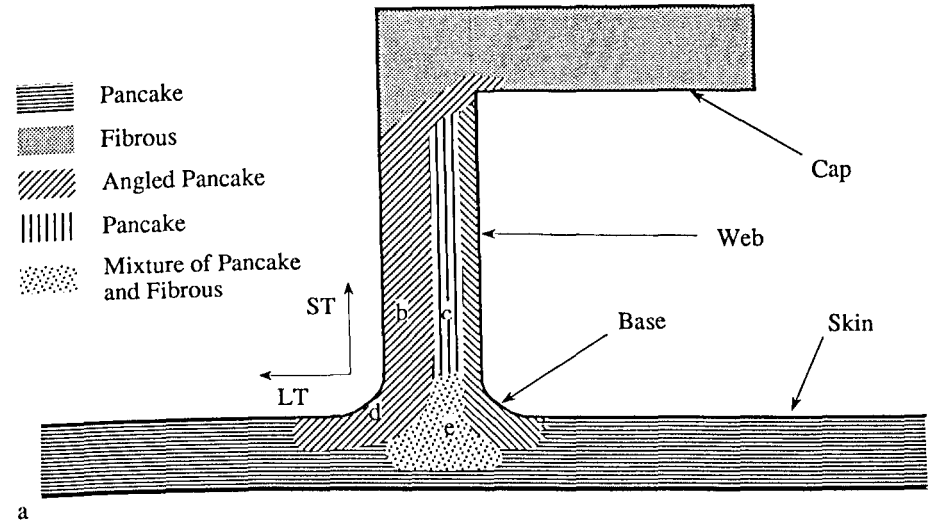

a

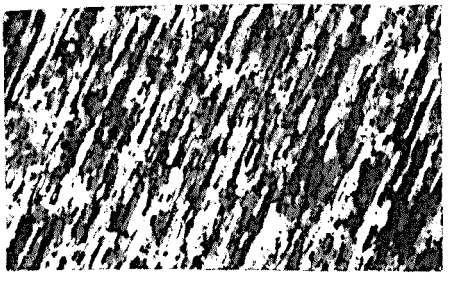

b

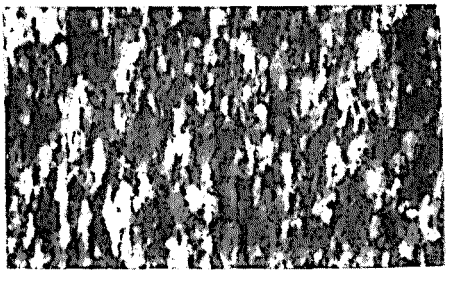

c

d

e

50 μm

Figure 1. Variations in grain morphology across a 2090 near net shape extrusion. Cross-section is perpendicular to the extrusion axis, or L direction. Tensile tests were conducted on the cap, web, base and skin in various orientations.

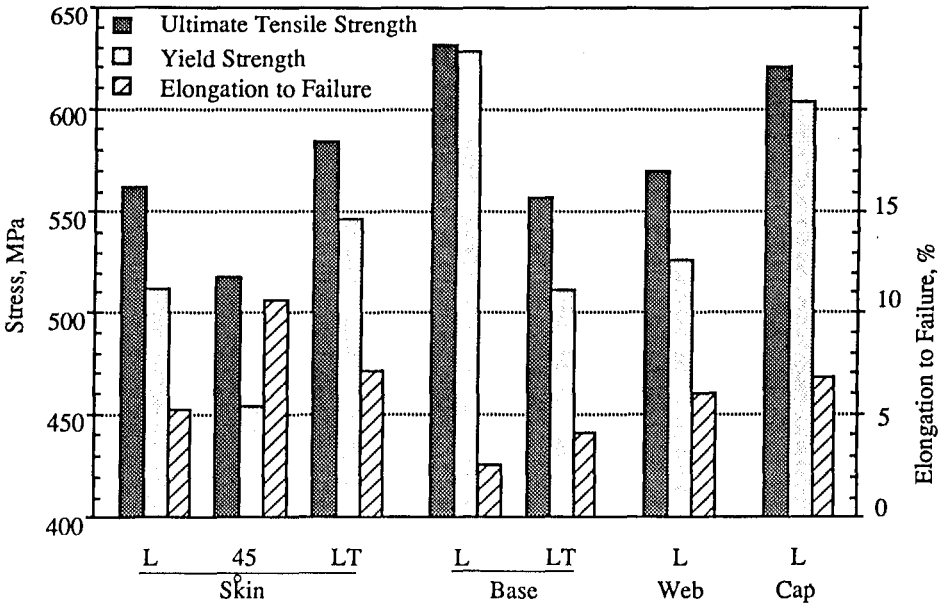

Figure 2. Strength and elongation to failure as a function of location and orientation within the extruded cross-section.

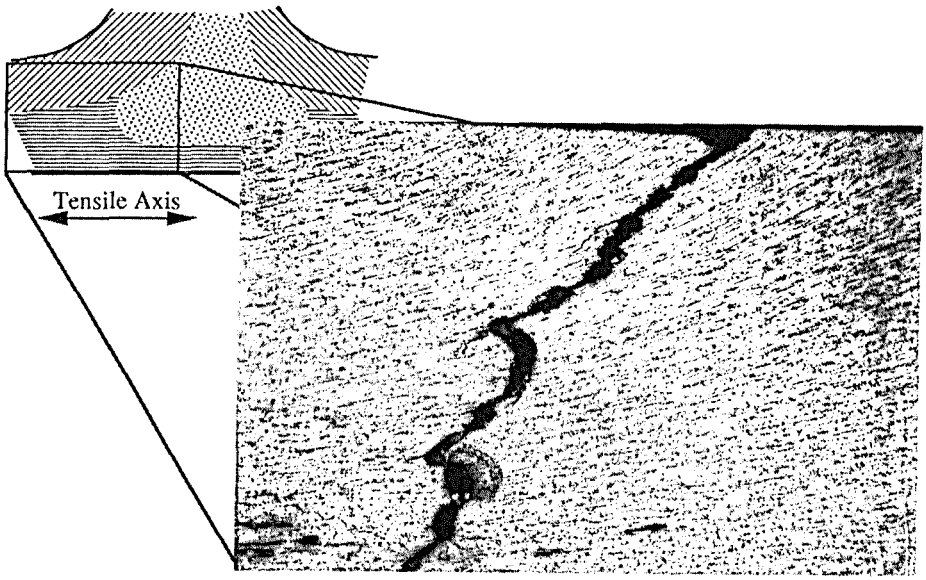

Figure 3. Macroscopic failure of an LT base specimen. The slant fracture path follows the local orientation of the grain structure around fillet.

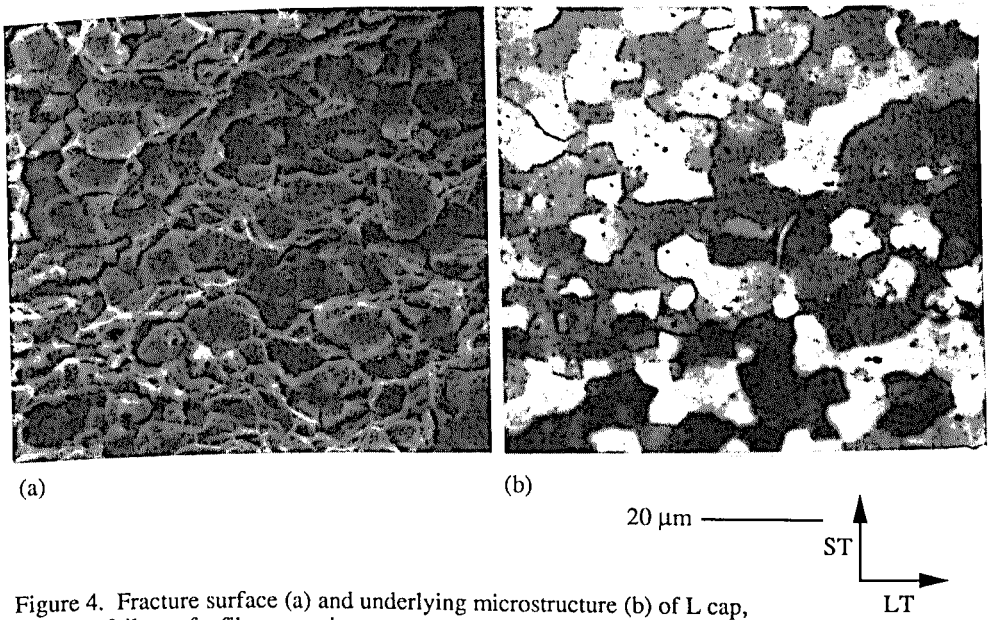

Figure 4. Fracture surface (a) and underlying microstructure (b) of L cap, showing failure of a fibrous grain structure.

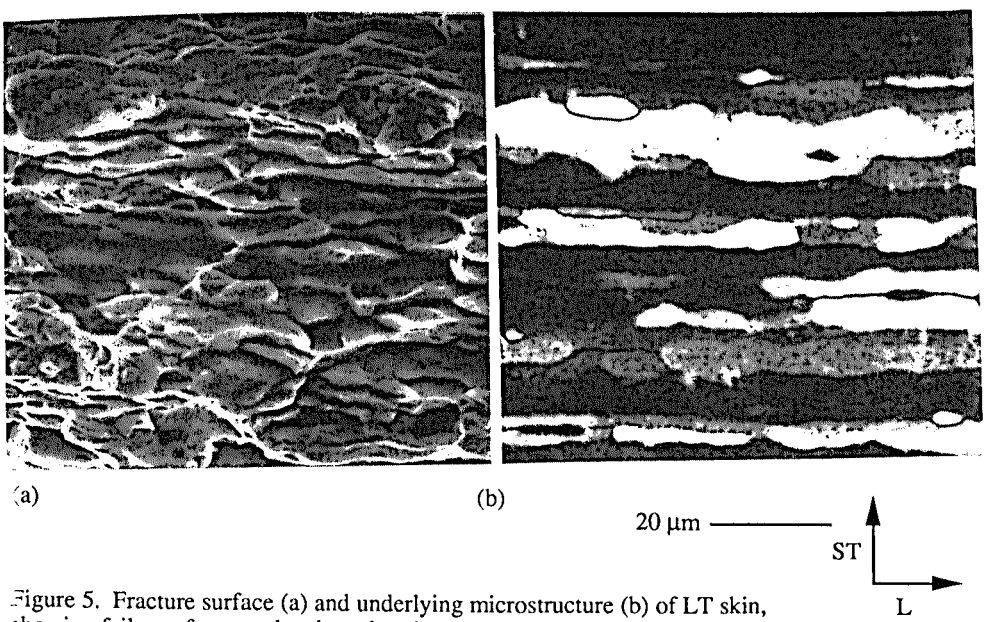

Figure 5. Fracture surface (a) and underlying microstructure (b) of LT skin, showing failure of a pancake-shaped grain structure.